

POLARIZED LINE PROFILES AS DIAGNOSTICS OF CIRCUMSTELLAR GEOMETRY IN TYPE IIN SUPERNOVAE

Jennifer L. Hoffman^{1,2}

RESUMEN

Las supernovas de Tipo IIn poseen firmas espectrales que indican una interacción intensa entre el material eyectado de la supernova y el material circunestelar denso previamente expulsado por la estrella en los episodios de pérdida de masa antes de la explosión. Mediante el estudio de esta interacción se pueden obtener pistas de la naturaleza de los progenitores del Tipo IIn y de la historia de las pérdidas de masa. En particular, los espectros de polarización de los Tipos IIn muestran polarizaciones complejas de líneas y características con el ángulo de posición que surgen como una combinación de efectos geométricos y ópticos. He construido un código de Monte Carlo que simula la transferencia de la línea de $H\alpha$ a través de los cascarones circunestelares con varias configuraciones geométricas y características ópticas. La superposición de las componentes de las líneas anchas y delgadas producidas en las diferentes regiones del ambiente circunestelar y modificadas por scattering de electrones y de líneas, absorción de hidrógeno, emisión térmica, efectos geométricos y del ángulo de visión dan una variedad de formas en las líneas polarizadas en los espectros modelo. Las comparaciones de estos resultados con las observaciones recientes de alta calidad espectropolarimétricas de las supernovas de Tipo IIn sugieren que un modelo de región de choque entre la fotosfera de la supernova y el cascarón circunestelar es necesario para producir las líneas de emisión polarizadas estrechas en la longitud de onda en reposo del $H\alpha$ vistas en algunas IIn's. Más aún, los resultados de los modelos apuntan hacia otras características en los perfiles de líneas polarizadas que pueden ser usados para acotar las características del material circunestelar de estos intrigantes objetos. La utilidad del código será extendida por el tratamiento de los efectos Doppler debido a la expansión de la región de scattering circunestelar, tales como aquella que caracteriza a los perfiles $H\alpha$ polarizados de la SN 1997eg Tipo IIn.

ABSTRACT

Supernovae of Type IIn possess spectral signatures that indicate an intense interaction between the supernova ejecta and surrounding dense circumstellar material cast off by the star in pre-explosion mass-loss episodes. Studying this interaction can yield clues to the nature of Type IIn progenitors and their mass loss history. In particular, polarization spectra of Type IIn's show complex line polarization and position angle features that arise from a combination of geometrical and optical effects. I have constructed a Monte Carlo code that simulates the transfer of the $H\alpha$ line through circumstellar shells with various geometrical configurations and optical characteristics. The superposition of broad and narrow line components produced in different regions of the circumstellar environment and modified by electron and line scattering, hydrogen absorption, thermal emission, and geometrical and viewing angle effects gives rise to a variety of polarized line shapes in the model spectra. Comparison of these results with recent high-quality spectropolarimetric observations of Type IIn supernovae suggests that a model "shock" region between the supernova photosphere and the circumstellar shell is necessary to produce the narrow polarized emission features at the rest wavelength of $H\alpha$ seen in some IIn's. Further model results point toward other features in the polarized line profile that can be used to constrain the characteristics of the circumstellar material in these intriguing objects. The code's usefulness will be extended by the treatment of Doppler effects due to expansion of the circumstellar scattering region, such as those that characterize the polarized $H\alpha$ profiles of the Type IIn SN 1997eg.

Key Words: CIRCUMSTELLAR MATTER — METHODS: NUMERICAL — POLARIZATION — RADIATIVE TRANSFER — STARS: MASS LOSS — SUPERNOVAE

1. INTRODUCTION

Our understanding of supernovae (SNe) has broadened in recent years to include the recognition that both the thermonuclear and the core-collapse

¹Department of Astronomy, University of California at Berkeley, 601 Campbell Hall, Berkeley, CA 94720-3411, USA (jhoffman@astro.berkeley.edu).

²NSF Astronomy & Astrophysics Postdoctoral Fellow.

types of these stellar explosions are inherently aspherical phenomena (e.g., Kozma et al. 2005; Burrows et al. 2006). Observations of net continuum polarization in both supernova (SN) types have provided key evidence of the intrinsic asymmetry of SN ejecta (e.g., Wang 2001; Leonard et al. 2006). Many SNe also display line polarization features in addition to broadband continuum polarization; these line effects are often more complex than simple depolarization by complete scattering redistribution, and they can provide specific clues to the nature of SN ejecta and their surrounding circumstellar media (e.g., Wang 2004; Leonard et al. 2005). However, line polarization can be produced by a combination of many different optical and geometrical effects, so its interpretation is not straightforward. Detailed radiative transfer modeling (as in Kasen et al. 2003) is often the best way to understand the effects that give rise to polarized lines in SN spectra. In the case of Type IIn (“narrow-line”; Filippenko 1997) supernovae, the situation is complicated by the presence of circumstellar material (CSM) surrounding the SN ejecta that becomes excited by the UV and X-ray photons from the SN explosion. Line polarization signatures in Type IIn SNe are superpositions of those arising from the ejecta and those arising from the CSM. Disentangling the two can be difficult but worthwhile, as it allows us to probe the nature and structure of the CSM to an extent not possible with spectroscopy alone (Leonard et al. 2000a; Wang 2001). Since the CSM of a Type IIn supernova most likely represents material ejected by the progenitor star, studying its geometrical and optical characteristics provides a link to the mass-loss episodes and stellar winds of massive stars in their late stages of evolution.

2. CODE

I have developed a Monte Carlo radiative transfer code called *SLIP* (for Supernova Line Polarization) that simulates the ways polarized line profiles are created in Type IIn supernovae. *SLIP* uses the three-dimensional spherical polar grid structure described by Whitney & Wolff (2002); it tracks virtual photons as they arise from a model SN photosphere and scatter in a circumstellar density distribution with wavelength-dependent emission, absorption, and scattering characteristics. Similar codes have enjoyed success in analyzing related scenarios such as hot star envelopes with aspherical wind geometries (Harries 2000) and ejecta-hole configurations in SNe Type Ia (Kasen et al. 2004). Unlike most previous codes that treat SN line polarization

(e.g., Höflich 1995), *SLIP* does not assume that line scattering is depolarizing; it also does not rely on the Sobolev approximation, but instead performs full radiative transfer in regions of high optical depth. It is thus able to probe in detail the polarized line profiles that may arise from interaction with the circumstellar material. Another advantage to this method is that it can simulate emission not only from a central source but also from extended regions such as the warm CSM (see below). However, the code is still in the early stages of development, and does not include any Doppler effects from the expanding circumstellar material; this limits the extent to which we can compare model outputs to observed line profiles, but the stationary case is a useful first approximation, especially in cases of low CSM velocity.

In the models presented here, a finite spherical source of photons at the center of the grid represents the “photosphere” of the SN ejecta, while two scattering regions surrounding the ejecta represent the warm, stationary CSM and a shock-heated region interior to the CSM, formed by its interaction with high-velocity SN material. Initially unpolarized photons are emitted from the surface of the photosphere with the synthetic $H\alpha$ P Cygni profile from a Type IIP supernova, produced with the *PHOENIX* stellar atmosphere code (Hauschildt et al. 1999). In the hot shock region, I assume only a narrow line is emitted, with a line width of < 80 km/s; this is similar to the widths of the narrow hydrogen lines in the Type IIn SN 1997eg (7–40 km/s) observed by Salamanca (2002). I do not directly simulate heating of the CSM by emission from the supernova, but rather choose a CSM temperature and emit photons from the volume of the region with the expected thermal continuum and line spectra of hydrogen, assuming Case B LTE (Osterbrock 1989). All photons then scatter within the CSM via electron scattering; the optical depth of the scattering region is also chosen as an input parameter. I also implement wavelength-dependent free-free and free-bound absorption effects as in Wood et al. (1996). Photons within the Doppler core of the line (Lang 1999) experience an additional bound-bound opacity; those absorbed by H atoms in this way are subsequently re-emitted coherently and isotropically.

When the code is run, *SLIP* emits photons sequentially from the photosphere, shock region, and CSM and follows each until it becomes absorbed or exits the system; at each scattering event, the code updates the photon’s Stokes parameters. Photons that exit the model system are binned by outgoing angle and the Stokes parameters are summed approx-

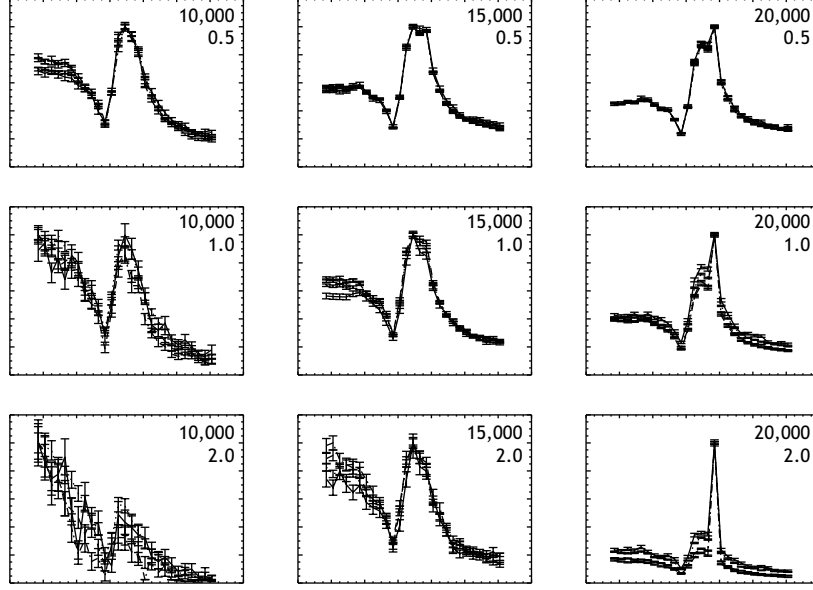


Fig. 1. Representative sample of the model flux grid described in § 3. All models shown here have ellipsoidal circumstellar density distributions; none includes emission from the shock region. In the individual panel labels, the upper number indicates the CSM temperature in Kelvin and the lower indicates the CSM optical depth. Each panel spans a wavelength range from 5800 Å to 7200 Å; each spectrum is normalized to its own peak flux. Four profiles are plotted in each panel, representing viewing angles of 3°, 35°, 66°, and 89°. Model A (Table 1) is depicted in the middle right panel.

priately in each bin. Thus each simulation produces a full three-dimensional model whose H α flux and polarization spectra can be “viewed” from any desired direction.

3. MODEL RESULTS

I have created a grid of 144 models spanning two CSM geometries (ellipsoids and toroids of similar sizes); CSM optical depths from 0.5 to 2; CSM luminosities from 1–20% of the photospheric luminosities; and CSM temperatures from 10,000 K to 20,000 K. Emission from the shock region was either included at 10% of the photospheric luminosity or excluded completely. In order to keep computing times reasonable, these models included only 1.8×10^7 photons each, enough to build up good signal in the flux spectrum but not the polarization spectrum. Since the goal was to match general features in both the flux and polarized flux, I used this grid to constrain parameter space for more computationally-intensive code runs including polarization. Figure 1 depicts results for nine representative models in the flux grid; it shows that significant differences in the line profiles arise for even small variations in optical depth and temperature of the scattering region.

With the flux grid complete, I compared the simulated H α profiles with observed H α profiles of Type

TABLE 1
REPRESENTATIVE MODEL PARAMETERS

Parameter	Model A	Model B
CSM geometry	ellipsoid	toroid
CSM optical depth	1.0	2.0
L_{CSM}/L_{phot}	0.01	0.1
L_{shock}/L_{phot}	0.0	0.1
CSM temperature	20,000 K	15,000K

IIn supernovae to determine which simulations to repeat for better signal in the polarized flux. This process is still underway, and the results will be published in an upcoming contribution. Here I present two representative simulations, Model A and Model B, that produce similar H α flux spectra but have quite different polarization behavior. Each included 1.6×10^9 photons, divided among 768 processors of the Seaborg parallel computing facility at the National Energy Research Scientific Computing Center (NERSC) at the Lawrence Berkeley Laboratory. Table 1 compares the parameters of these two models, while Figure 2 compares their H α line profiles at a range of viewing angles with the profile observed for

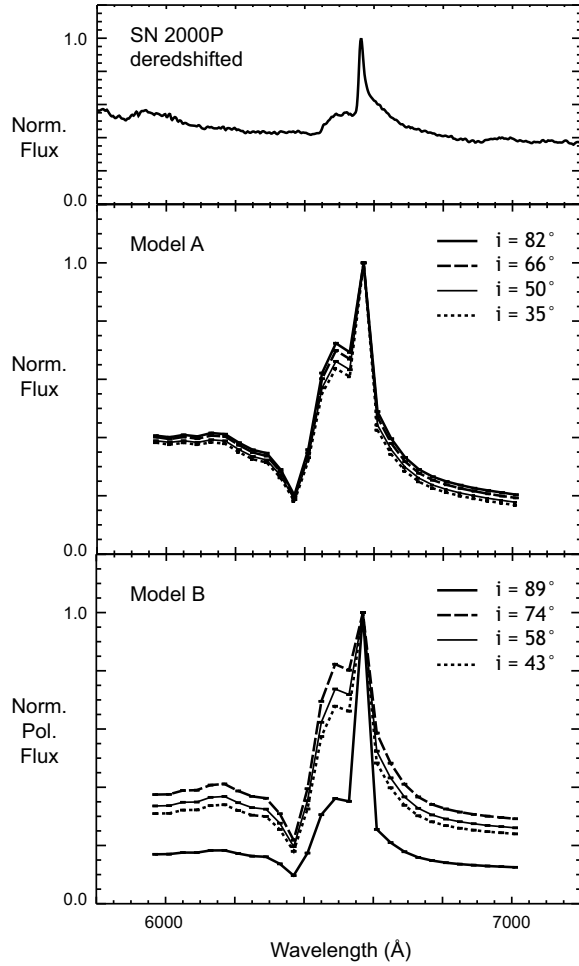


Fig. 2. (*top*) De-redshifted $H\alpha$ total flux profile of SN 2000P at day 13 post-discovery (A. V. Filippenko 2004, private comm.). (*middle*) Simulated $H\alpha$ profile arising from Model A (Table 1) at varying inclination angles from the polar axis. (*bottom*) As in the middle panel, but for Model B. All line profiles have been normalized to 1 at the rest wavelength of 6563 Å.

SN 2000P (A. V. Filippenko 2004, private communication) at day 13 post-discovery. Both models can reproduce the general observed line shape of a narrow emission “spike” superposed on a broad base (I note that due to the *SLIP* code’s limitation to stationary scattering regions, the width of the broad line in these models arises solely from the input IIP spectrum arising from the model SN photosphere). While the profiles produced by Model A (the ellipsoid) are nearly completely degenerate in viewing angle, Model B (the toroid) shows a significant variation with viewing angle, particularly in the strength of the “spike” relative to the broad base. Examination of the other models in the grid suggests that the

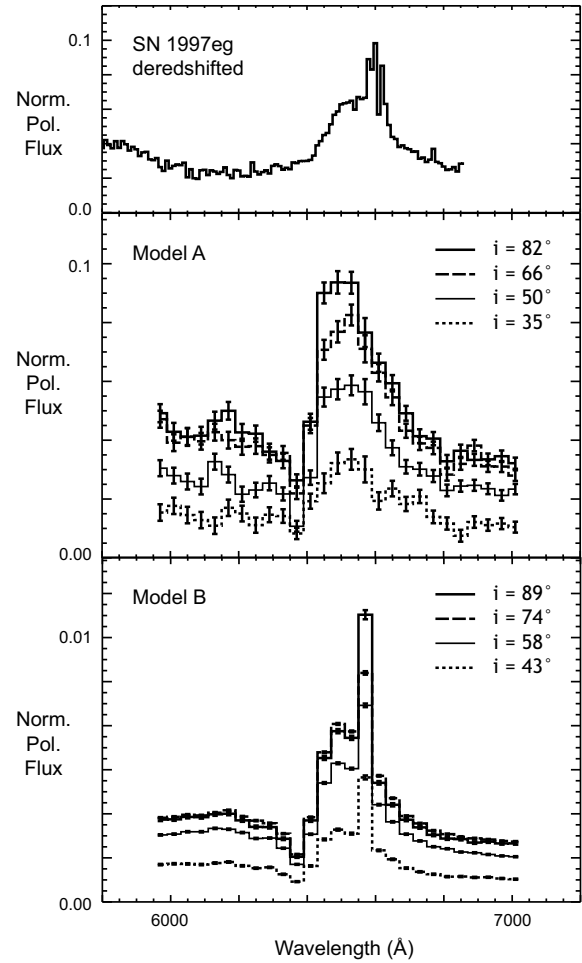


Fig. 3. (*top*) De-redshifted $H\alpha$ polarized flux profile of SN 1997eg at day 44 post-discovery (Hoffman 2006). (*middle*) Simulated $H\alpha$ polarized flux profile arising from Model A (Table 1) at varying inclination angles from the polar axis. (*bottom*) As in the middle panel, but for Model B. All polarized line profiles have been normalized to 1 at the rest wavelength of 6563 Å.

differences between these two families of $H\alpha$ profiles are mainly due to the difference in CSM geometry between these two models.

In Figure 3 I present the $H\alpha$ line profiles of Models A and B in polarized flux and compare them with that of the Type II in SN 1997eg (Leonard et al. 2000b; Hoffman 2006) at 44 days post-discovery. Recall that polarized flux is percent polarization multiplied by total flux; these profiles thus represent the spectra of the scattered light in each model. In polarized light the $H\alpha$ profiles look quite different than in direct light. The degeneracies that characterized Model A in direct light (Figure 2) have been lifted, raising the possibility of using polarized line profiles

to diagnose inclination angle in cases of known geometry. The two models now show line profiles quite distinct from each other; in particular, Model A produces no narrow “spike” at the rest wavelength in the polarized flux, while Model B preserves the spike. Examination of the other models in the flux grid suggests that this difference is due not to the difference in geometrical structure of the CSM between the two models, but rather to the presence of shock emission in Model B. Evidently the diffuse thermal emission from the CSM is sufficient to create a narrow spike in direct light, but in polarized light this feature requires a more directional source of narrow-line photons (the shock region). Photons from this region are more likely to scatter and become polarized while traversing the CSM than are photons that arise within its volume. However, Model B does not match the observed magnitude of polarization in SN 1997eg, most likely due to its larger CSM optical depth.

I continue to investigate these model results to pinpoint further diagnostics for geometry, temperature, and optical depth of the circumstellar material and the presence of a narrow-line “shock” region in Type IIn ejecta. More detailed analysis will be published in an upcoming contribution.

4. OBSERVED $H\alpha$ LINE PROFILES OF SN 1997EG

As mentioned in §2, my current *SLIP* code has the limitation of treating only stationary scattering regions, when in fact one expects velocity effects to be quite prominent contributors to line profiles in polarized light. Here I present two examples of line polarization effects in a Type IIn supernova that cannot yet be reproduced by the code but provide key information regarding the geometry of the circumstellar material. Along with collaborators at San Diego State University and UC Berkeley, I have studied the polarization spectrum of SN 1997eg (whose $H\alpha$ polarized flux profile is shown in Figure 3); our full analysis will appear in Hoffman (2007).

Figure 4 compares the $H\alpha$ line profiles of SN 1997eg in total flux (nearly all direct light) and scattered light at day 16, day 44, and day 93 post-discovery. Although the continuum polarized flux is only about 2% of the total at each epoch, I have normalized both spectra to the same scale for comparison of the line profiles. At all epochs the polarized lines are broader than the unpolarized lines. This implies first that the scattering region has a different geometry from that of the broad-line emission region, and second that the scattering region is expanding

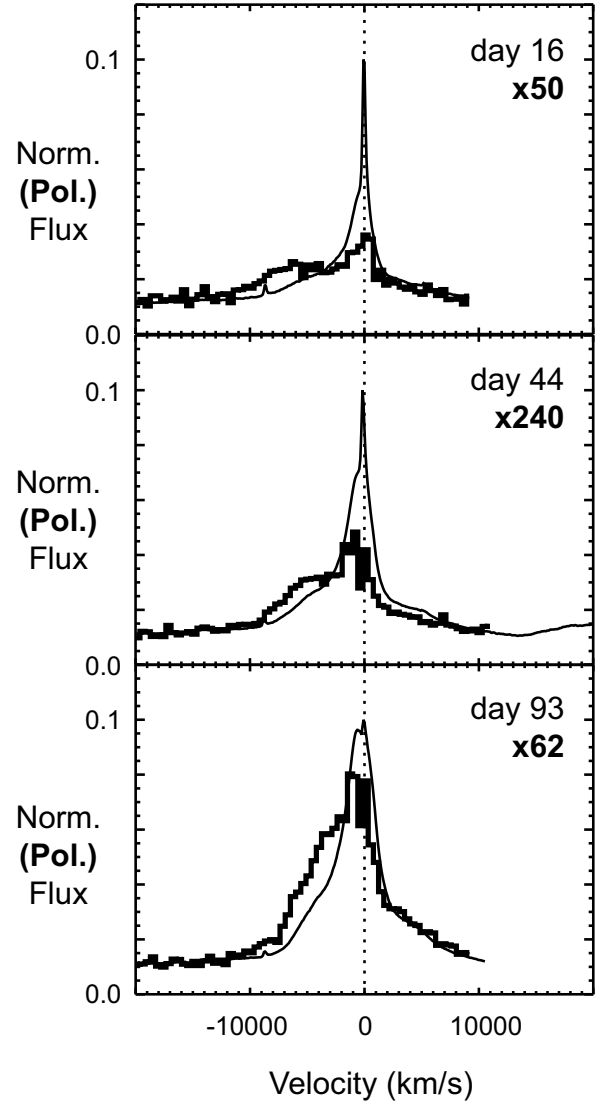


Fig. 4. Line profiles of the $H\alpha$ line of SN 1997eg in total flux (*narrow smooth lines*) and polarized flux (*thick binned lines*) at each of the three epochs of spectropolarimetry (days 16, 44, and 93 post-discovery). Total flux spectra have been normalized to their respective line peaks. Each polarized flux spectrum has been binned to a resolution of 10 Å and multiplied by the same normalizing factor as its corresponding total flux spectrum, then by an additional factor shown in each frame to facilitate direct comparison of the line shapes.

at a higher velocity than the emission region. The fact that the polarized lines are broader only in the blue wing suggests the redshifted side of the scattering region may be self-occulted (or perhaps occulted by the SN ejecta) from our line of sight. If we postulate a flattened toroidal or disk-like geometry for the

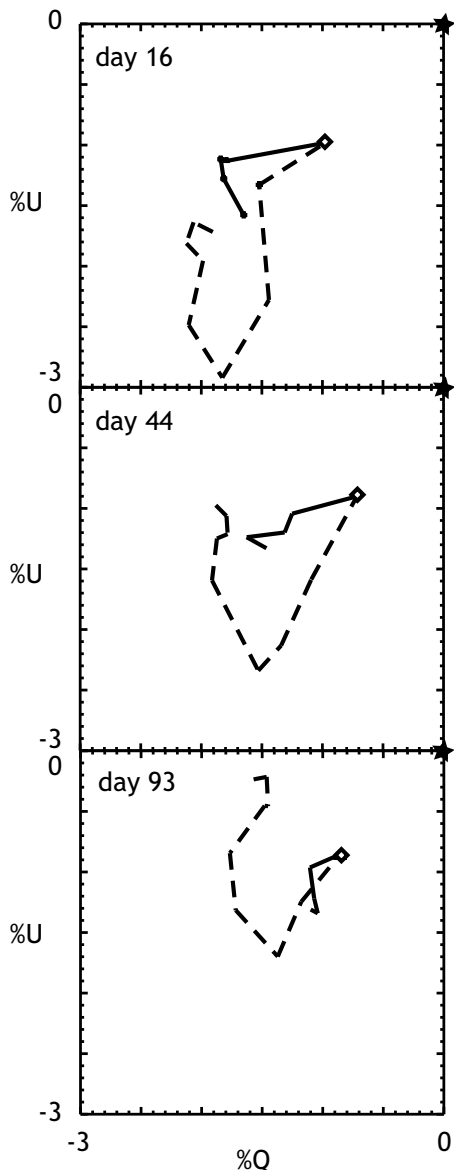


Fig. 5. Polarization profiles of the $H\alpha$ emission line of SN 1997eg in the $q-u$ plane for each of the three epochs of spectropolarimetry (days 16, 44, and 93 post-discovery). Data have been binned to a resolution of 50 \AA for clarity. Dashed lines represent negative (blueshifted) velocities; solid lines represent positive (redshifted) velocities. In each frame, the rest wavelength is shown with an open diamond and the origin of the plot is in the upper right corner.

scattering region, this result can help place limits on the spatial inclination of the CSM configuration.

In Figure 5 I plot the polarized $H\alpha$ lines of the three epochs in $q-u$ space, a technique that allows visualization of all polarimetric information at once.

Not only does the magnitude of polarization change across the $H\alpha$ line at all epochs in SN 1997eg, but the position angle changes as well, in a manner that creates closed “loops” in the $q-u$ plane (distinct from “knots,” which characterize a constant polarization signal with wavelength, and from straight lines, which arise from simple envelope expansion or line depolarization). This implies that the scattering region polarizing the $H\alpha$ line has a different orientation than the one polarizing the continuum light (presumably the SN ejecta). In particular, the “loop” shape implies that the symmetry axes of the two regions are different, and that the CSM occults the SN ejecta in such a way as to create an asymmetry in the Stokes parameters across the line center. In the models of Kasen et al. (2003), such $q-u$ loops are general features of two-axis systems; I postulate a toroidal geometry such as that shown in these authors’ Figures 14 and 15.

I note that the preceding results are both independent of interstellar polarization effects, for which the observed data have not been corrected. Similar complex behavior in the $H\beta$ and $\text{He I } \lambda 5876$ lines in the SN 1997eg spectrum is discussed fully in the upcoming article. The results combine to suggest that SN 1997eg is characterized by ellipsoidal ejecta that polarize the continuum light and a flattened, disk-like CSM exterior to the ejecta that polarizes the hydrogen lines. The key conclusion is that the ejecta and the CSM have different axes of symmetry.

Multi-axis systems are becoming recognized as quite common in mass-loss scenarios. P Cyg (Nordieck et al. 2001; Meaburn 2001), η Car (Smith 2006), and VY CMa (Humphreys 2005) are examples of massive stellar systems in which the circumstellar material shows evidence for multiple mass-loss episodes along different axes. Our observations of polarized line profiles in SN 1997eg suggest that the geometry of an asymmetric SN explosion may, in turn, be unrelated to the geometry of the progenitor’s stellar wind or its mass eruptions. Continued refinements to the *SLIP* radiative transfer code will allow me to construct more detailed models of the CSM surrounding SN 1997eg and related objects, as well as further probing the nature both of Type II SN explosions and the eruptions that characterize their progenitor stars.

This research was supported by an NSF Astronomy & Astrophysics Postdoctoral Fellowship, AST-0302123, and by the National Energy Research Scientific Computing Center, US DOE Contract #DE-AC03-76SF00098. I thank my primary collaborators

Alex Filippenko at UC Berkeley, Peter Nugent at LBL, and Doug Leonard at San Diego State University, for their invaluable contributions.

REFERENCES

- Burrows, A., Livne, E., Dessart, L., Ott, C. D., & Murphy, J. 2006, *ApJ*, 640, 878
- Filippenko, A. V. 1997, *ARA&A*, 35, 309
- Harries, T. J. 2000, *MNRAS*, 315, 722
- Hauschildt, P. H., & Baron, E. 1999, *J. Comput. Appl. Math.*, 109, 41
- Hoffman, J. L. 2006, *The Circumstellar Environment of SN 1997eg* (<http://grammai.org/jhoffman/pubs/keck06.html>)
- Hoffman, J. L., Leonard, D. C., Chornock, R., Filippenko, A. V., Barth, A. J., Matheson, T., & Coil, A. 2007, *ApJ*, submitted
- Höflich, P. 1995, *ApJ*, 440, 821
- Humphreys, R. M., Davidson, K., Ruch, G., & Wallerstein, G. 2005, *AJ*, 129, 492
- Kozma, C., Fransson, C., Hillebrandt, W., Travaglio, C., Sollerman, J., Reinecke, M., Röpke, F. K., & Spyromilio, J. 2005, *A&A*, 437, 983
- Kasen, D. K., et al. 2003, *ApJ*, 593, 788
- Kasen, D. K., Nugent, P., Thomas, R. C., & Wang, L. 2004, *ApJ*, 610, 876
- Lang, K. R. 1999, *Astrophysical Formulae*, Volume I (3rd ed; Berlin: Springer-Verlag)
- Leonard, D. C., Filippenko, A. V., Barth, A. J., & Matheson, T. 2000a, *ApJ*, 536, 239
- Leonard, D. C., Filippenko, A. V., & Matheson, T. 2000b, in *AIP Conf. Proc.* 522, *Cosmic Explosions*, ed. S. S. Holt & W. W. Zhang (Melville: AIP), 165
- Leonard, D. C., Li, W., Filippenko, A. V., Foley, R. J., & Chornock, R. 2005, *ApJ*, 632, 450
- Leonard, D. C., et al. 2006, *Nature*, 440, 505
- Meaburn, J. 2001, in *ASP Conf. Proc.* 233, *P Cygni 2000: 400 Years of Progress*, ed. M. de Groot & C. Sterken (San Francisco: ASP), 253
- Nordsieck, K. H., et al. 2001, in *ASP Conf. Proc.* 233, *P Cygni 2000: 400 Years of Progress*, ed. M. de Groot & C. Sterken (San Francisco: ASP), 261
- Osterbrock, D. E. 1989, *Astrophysics of Gaseous Nebulae and Active Galactic Nuclei* (Mill Valley, CA: University Science Books)
- Salamanca, I., Terlevich, R. J., & Tenorio-Tagle, G. 2002, *MNRAS*, 330, 844
- Smith, N. 2006, *ApJ*, 644, 1151
- Wang, L., Baade, D., Höflich, P., Wheeler, J. C., Kawanabata, K., & Nomoto, K. I. 2004, *ApJ*, 604, L53
- Wang, L., Howell, D. A., Höflich, P., & Wheeler, J. C. 2001, *ApJ*, 550, 1030
- Whitney, B. A., & Wolff, M. J. 2002, *ApJ*, 574, 205
- Wood, K., Bjorkman, J. E., Whitney, B., & Code, A. 1996, *ApJ*, 461, 847